Viscoplastic Displacement Flow in a Rotating Pipe

Nasim Kazemi, Soheil Akbari, David Vidal, Seyed Mohammad Taghavi

Dept. of Mechanical Engineering –Polytechnique Montréal, Montréal, QC, Canada

Dept. of Chemical Engineering – Université Laval, Québec, QC, Canada

Introduction

Industrial motivations:

- There has been an increase of 56% in energy consumption from 2010 to 2040.
- The world is still highly dependent on fossil fuels.
- Canada requires enhancing oil & gas industries as one of the global energy providers.

Applications of displacement flows in the oil and gas industry:

- Primary well cementing
- Plug and abandonment

Advantages of primary well cementing:

- Creating hydraulic seal and zonal isolation
- Preventing fluids' contamination
- Supporting well and casing mechanically
- Protecting water-producing zones
- Preventing corrosion of the casing

Different stages of primary well cementing:

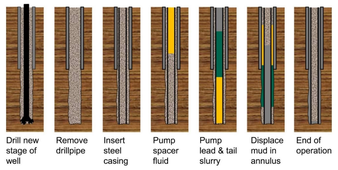

Figure 1 Schematic of the stages of mud removal in primary well cementing [1].

What is the benefit of adding axial rotation in well cementing?

There has been a recent interest to propose robust methods to improve the displacement efficiency in the primary cementing process, an example of which is applying the casing (pipe) rotation. There are preliminary studies showing that the casing rotation increases the displacement efficiency in this process [1-5]. However, despite the existence of various types of casing heads and special adaptors, capable of the casing axially rotation (with a moderate speed of up to 60 rpm) to maximize the displacement efficiency, this method is not used widely. One reason is due to the lack of theoretical and fundamental knowledge about the effects of rotation in viscoplastic displacement flows. That is why we are partly motivated by studying the effects of the casing axial rotation on viscoplastic displacement flows, with potential applications in the primary cementing process. We are focusing on how rotation may affect the displacement flow behavior when the cement slurry is injected into the casing and is displacing Newtonian fluids which are available in the casing.

Properties of cement slurry:

Generally, cement slurry behaves as a non-Newtonian fluid. For oilfield purposes, it is mainly considered a viscoplastic fluid. Cement slurry shows a variety of complex flow behaviors. Thus, there are several models to predict cement behavior. However, for oilfield purposes, mainly Herschel-Bulkley model is considered [6]. It is described as below.

Herschel-Bulkley model: $\begin{cases} \hat{\tau} = \hat{\tau}_y + \hat{\kappa}\hat{\dot{\gamma}}^n & \hat{\tau} > \hat{\tau}_y \\ \hat{\dot{\gamma}} = 0 & \hat{\tau} \le \hat{\tau}_y \end{cases}$

Literature Review

Authors	Flow type	Fluids types	Geometry	Inclination	Geometry Movement	*At*	*m*	Approach
Lyu ***et al.*** **2018 [2]**	Exchange	Newtonian	Pipe, $\hat{H} = 3\ m$, $\hat{R} = 9.5\ mm$	65 – 85 degrees from vertical	0-7.33 rad/s	0.0035 – 0.01	1	Experimental & numerical
Amiri *et al.* 2018 [3]	Imposed	Newtonian	Pipe, $\hat{H} = 3\ m$, $\hat{R} = 9.5\ mm$	Vertical	oscillation	(0.001-7) $\times 10^{-2}$	1	Experimental
Lyu & Taghavi 2020 [4]	Imposed	Newtonian	Pipe, $\hat{H} = 3\ m$, $\hat{R} = 9.5\ mm$	60 – 83 degrees from vertical	0-7.33 rad/s	(1.5, 5.5, 10) $\times 10^{3}$	1	Experimental
Lyu & Taghavi 2020 [5]	Imposed	Yield stress displaced fluid	Pipe, $\hat{H} = 3\ m$, $\hat{R} = 9.5\ mm$	60 – 80 degrees from vertical	0-6.28 rad/s	0.0035-0.02	Large	Experimental

Objectives

1. Effects of **yield stress** in a *stationary* vertical pipe:
   - Bingham number
   - Froude number
   - Reynolds number
2. Effects of **pipe axial rotation** and **yield stress** in an *axially rotating* vertical pipe:
   - Rossby number
   - Bingham number
   - Reynolds number
3. Effects of **pipe axial rotation** in an *axially rotating* inclined pipe:
   - β (pipe inclination from vertical)
   - Rossby number
4. Effects of **pipe axial rotation** and **yield stress** in an *axially rotating* inclined pipe:
   - β
   - Bingham number
   - Froude number
   - Reynolds number
   - Rossby number

Experimental approach

The experimental setup is shown both schematically and in real.

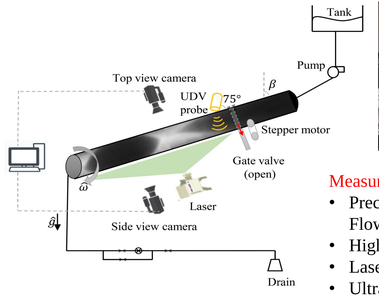

Figure 2 Schematic of experimental setup.

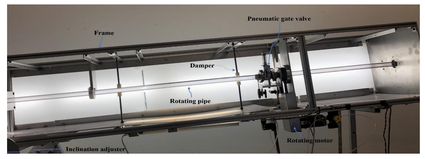

Figure 3 Real experimental setup.

Measurement tools:

- Precious scale, Density meter, pH-meter, Rheometer, Flow meter.
- High speed camera
- Laser induced Fluorescence (LIF)
- Ultra doppler velocimetry (UDV)
- Particle image velocimetry (PIV)

Ranges of variables

Ranges of dimensional and dimensionless variables of our experiments are listed below.

Operational Dimensional numbers	Series 1 Effects of $\hat{\tau}_y$ in a vertical stationary pipe	Series 2 Effects of $\hat{\tau}_y$ & $\hat{\omega}$ in a vertical rotating pipe	Series 3 Effects of β in an inclined rotating pipe	Series 4 Effects of $\hat{\omega}$ & $\hat{\tau}_y$ in an inclined rotating pipe
$\hat{\omega}\ (rad/s)$	0	0, 3.14, 6.30, 9.4	0-9.4	0, 3.14, 6.30, 9.4
$\hat{V}_0\ (mm/s)$	5-1000	5-1000	5-1000	5-1000
$\hat{\rho}_L\ (kg/m^3)$	997	997	997	997
$\hat{\rho}_H\ (kg/m^3)$	1007	1007	1007	1007
$\hat{\mu}_L\ (Pa.s)$	10^{-3}	10^{-3}	10^{-3}	10^{-3}
$\hat{\mu}_H\ (Pa.s)$	0.49-0.58	0.49-0.58	0.49	0.49-0.58
$\hat{\tau}_y\ (Pa)$	~ 0.17, 2, 4, 8, 10	~ 0.17, 2, 4, 8, 10	~ 4	~ 0.17, 2, 4, 8, 10

Operational Dimensionless numbers	Series 1 Effects of $\hat{\tau}_y$ in a vertical stationary pipe	Series 2 Effects of $\hat{\tau}_y$ & $\hat{\omega}$ in a vertical rotating pipe	Series 3 Effects of β in an inclined rotating pipe	Series 4 Effects of $\hat{\omega}$ & $\hat{\tau}_y$ in an inclined rotating pipe
β	0	0	0, 30, 60, 75	0-75
n	0.1-1	0.1-1	0.1-1	0.1-1
At	0.49×10^{-2}	0.49×10^{-2}	0.49×10^{-2}	0.49×10^{-2}
Rb	-	0.05-∞	0.05-∞	0.05-∞
Fr or Fr_m	0.29-108.14	0.29-108.14	0.30-∞	0.30-∞
Re	1.62-1736.21	1.62-1736.21	1.62-1736.21	1.62-1736.21
m	$(0.03\text{-}0.6)\times10^{-2}$	$(0.03\text{-}0.6)\times10^{-2}$	$(0.01\text{-}0.3)\times10^{-2}$	$(0.03\text{-}0.6)\times10^{-2}$
Bn	0.44×10^{-2}-2.4	0.44×10^{-2}-2.4	0.24	0.44×10^{-2}-2.4

Numerical approach

Geometry & Boundary conditions:

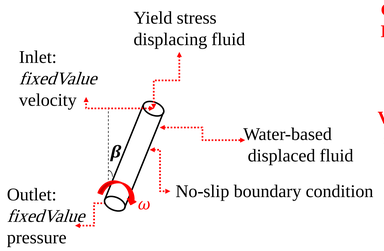

Governing Equations:

$$\frac{\partial c}{\partial \hat{t}} + \nabla \cdot (c\hat{u}) = 0$$
$$\nabla \cdot \hat{u} = 0$$
$$\frac{\partial \hat{\rho}\hat{u}}{\partial \hat{t}} + \nabla \cdot (\hat{\rho}\hat{u}\hat{u}) = -\nabla\hat{p} + \nabla.\hat{\tau} + \hat{\rho}\hat{g}$$

Viscoplastic displacing Fluid:
- Herschel-Bulkley model
- Regularized model

Solution:
- OpenFOAM
- InterFoam solver
- VOF methods for interface tracking
- Compute Canada

Preliminary results

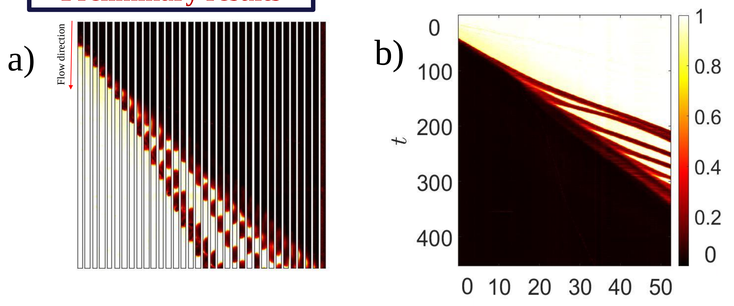

Figure 4 Time evolution of fluids displacement in an experiment (a) and spatiotemporal diagrams of the depth-averaged concentration field (b) for Re=7811, n=1 , Fr=0.1914, Bn=0.0035 in the vertical position. The color bar shows concentration values. 0 indicates pure heavy fluid and 1 shows the light one.

Let's describe a typical experiment of the displacement flow. Fig. 4.a shows the snapshots of a typical experiment, with time increasing from left to right. The fluids are initially separated by a gate valve. After opening the gate valve, the heavy fluid enters the flow domain below the gate valve and penetrates into the light fluid. To simplify our understanding of how the flow develops, we have identified the following phases during the advancement of the heavy fluid under the injection inlet, into the light fluid:

- First, the dyed heavy fluid uniformly enters the flow domain, which is previously filled with transparent light fluid.
- As the heavy fluid is injected progressively, it comes down in a piston-like flow pattern.
- Suddenly, a small amount of the front is separated from the whole injected fluid. It happens as the result of the fact that buoyancy force overcomes the inertial and the yield stresses of the displacing fluid.
- This happens continuously until when the two competitive upward forces become strong enough to compete with the buoyancy force.

Fig. 4.b depicts the spatiotemporal diagram of the depth-averaged concentration field of heavy fluid and describes how the concentration is changing in the length of the pipe over the time of the experiment. The horizontal axis is made dimensionless with the radius of the pipe and the vertical one with $\hat{V}_0/\hat{R}$. It is obvious that when separations occur, the concentration suddenly changes from about zero to around 1 and it is possible to count the number of separated pieces from the diagram. Furthermore, the velocity of the separated pieces can be measured from the slope of the related comparative boundaries of concentration profiles.

References

[1] A. Maleki and I. Frigaard, "Primary cementing of oil and gas wells in turbulent and mixed regimes," *J. Eng. Math.*, 2017.

[2] S. Lyu, M. Izadi, and S. M. Taghavi, "Exchange flows in axially rotating pipes," *Phys. Rev. Fluids*, 2020.

[3] A. Amiri, F. Larachi, and S. M. Taghavi, "Displacement flows in periodically moving pipe: understanding multiphase flows hosted in oscillating geometry," *Chem. Eng. Sci.*, 2017.

[4] S. Lyu and S. M. Taghavi, "Stratified flows in axially rotating pipes," *Phys. Rev. Fluids*, 2018.

[5] S. Lyu and S. M. Taghavi, "Viscoplastic displacements in axially rotating pipes," *J. Non-Newtonian. Fluid Mech.*, 2020.

[6] S. Akbari and S. M. Taghavi, "From breakup to coiling and buckling regimes in buoyant viscoplastic injections," *J. Fluid Mech.*, 2022.

Nomenclature

β	Pipe inclination angle	At	Atwood number	m	Viscosity ratio
$\hat{\dot{\gamma}}$	Shear rate, 1/s	Bn	Bingham number	n	Power law index
$\hat{\kappa}$	Consistency index, Pa.s^n	B_N	Newtonian Bingham number	$\hat{p}$	Pressure, Pa
$\hat{\mu}_H$	Dynamic viscosity of heavy fluid (Pa.s)	c	Depth-averaged concentration	Pe	Peclet number
$\hat{\mu}_L$	Dynamic viscosity of light fluid (Pa.s)	$\hat{D}_m$	Macroscopic diffusion coefficient, m^2/s	Re_t	Modified Reynolds number
$\hat{\rho}_H$	Density of heavy fluid, kg/m^3	Fr	Froude number	Rb	Rossby number
$\hat{\rho}_L$	Density of heavy fluid, kg/m^3	Fr_m	Modified Froude number	$\hat{R}$	Radius of the pipe, m
$\hat{\tau}$	Shear stress, Pa	$\hat{g}$	Standard acceleration of free fall, m/s^2	$\hat{V}_0$	Mean imposed velocity, m/s
$\hat{\tau}_y$	Yield stress, Pa	$\hat{H}$	Height of geometry, m	$\hat{W}$	Width of the geometry, m
$\hat{\omega}$	Rotational speed, rad/s	$\hat{L}$	Pipe length, m		

Acknowledgments

INNOVATION.CA CANADA FOUNDATION FOR INNOVATION | FONDATION CANADIENNE POUR L'INNOVATION

NSERC CRSNG

Chaires de recherche du Canada | Canada Research Chairs

Canada